crystals

MDPI

Article

Caysichite-(Y) from the Ploskaya Mountain (Kola Peninsula, Russia): Crystal-Structure Refinement and the Chemical Formula

Sergey V. Krivovichev [1,2,*], Victor N. Yakovenchuk [1,3], Olga F. Goychuk [1,3] and Yakov A. Pakhomovsky [1,3]

[1] Nanomaterials Research Center, Kola Science Center, Russian Academy of Sciences, Fersmana Str. 14, 184209 Apatity, Russia; v.yakovenchuk@ksc.ru (V.N.Y.); o.goychuk@ksc.ru (O.F.G.); y.pakhomovskiy@ksc.ru (Y.A.P.)
[2] Department of Crystallography, Institute of Earth Sciences, St. Petersburg State University, University Emb. 7/9, 199034 St. Petersburg, Russia
[3] Geological Institute, Kola Science Center, Russian Academy of Sciences, Fersmana Str. 14, 184209 Apatity, Russia
* Correspondence: s.krivovichev@ksc.ru

Abstract

The crystal structure of caysichite-(Y) from the Ploskaya Mt (Kola Peninsula, Russia) has been refined to R_1 = 0.051 for 4472 unique observed reflections. The mineral is orthorhombic, $Ccm2_1$, a = 13.2693(3), b = 13.9455(4), c = 9.7384(2) Å, V = 1802.06(8) Å^3, Z = 4. There are two M sites predominantly occupied by Y, but also including Ca and other rare earth elements (REEs). Both M sites are coordinated by eight O atoms to form distorted bicapped trigonal prisms. The crystal structure is based upon a three-dimensional framework formed by columns of MO_8 polyhedra and (CO_3) groups and double-crankshaft chains of SiO_4 tetrahedra running parallel to the *c*-axis. The topology of linkage of MO_8 polyhedra understood in terms of the M–M links shorter than 5 Å corresponds to the M network with the paracelsian (**pcl**) topology. The channels in the network are occupied by double-crankshaft Si chains and H_2O groups. The new general chemical formula of a caysichite-(Y)-type mineral can be written as $[Y_{2+2x-y'}Ca_{2-3x-y''}\square_{x+y'+y''}][Si_4O_{10}](HCO_3)_{3y'+2y''}(CO_3)_{3-3y'-2y''}\cdot(4-z)H_2O$, where $z \sim 0.2$; $x \leq 2/3$; $y' \leq 2/3$; $y'' \leq 1$; $3y'+2y'' \leq 2$. This general formula allows for several end-member formulas according to different x, y′ and y″ values: $(Y_2Ca_2)[Si_4O_{10}](CO_3)_3\cdot 4H_2O$ (x = y′ = y″ = z = 0), $(Y_2Ca\square)[Si_4O_{10}](HCO_3)_2(CO_3)\cdot 4H_2O$ (x = y′ = z = 0; y″ = 1), $(Y_{10/3}\square_{2/3})[Si_4O_{10}](CO_3)_3\cdot 4H_2O$ (y′ = y″ = z = 0; x = 2/3), $Ca_2Y_{4/3}\square_{2/3})[Si_4O_{10}](HCO_3)_2(CO_3)\cdot 4H_2O$ (x = y″ = z = 0; y′ = 2/3). The samples studied in this work have the compositions $(REE_{2.05}Ca_{1.87}\square_{0.18})[Si_4O_{10}](HCO_3)_{0.11}(CO_3)_{2.89}\cdot 3.8H_2O$ (x = 0.025, y′ = 0, y″ = 0.055) and $(REE_{2.25}Ca_{1.52}\square_{0.23})[Si_4O_{10}](HCO_3)_{0.21}(CO_3)_{2.79}\cdot 3.8H_2O$ (x = 0.125, y′ = 0, y″ = 0.115). The end-member formula most close to these compositions is $(Y_2Ca_2)[Si_4O_{10}](CO_3)_3\cdot 4H_2O$, which is different from the formula $(Ca,Yb,Er)_4Y_4(Si_8O_{20})(CO_3)_6(OH)\cdot 7H_2O$ currently adopted by the International Mineralogical Association but is generally identical to the formula $(Y,Ca)_4Si_4O_{10}(CO_3)_3\cdot 4H_2O$ proposed in the original study of the mineral. In order to resolve the problem of the caysichite-(Y) formula, additional studies of materials from different localities (and, especially, one from the holotype locality) are needed.

Keywords: rare earth minerals; crystal structure; caysichite-(Y); Kola Peninsula; silicate; carbonate; chemical formula

Academic Editor: Milena Rosić

Received: 22 August 2025
Revised: 5 September 2025
Accepted: 8 September 2025
Published: 9 September 2025

Citation: Krivovichev, S.V.; Yakovenchuk, V.N.; Goychuk, O.F.; Pakhomovsky, Y.A. Caysichite-(Y) from the Ploskaya Mountain (Kola Peninsula, Russia): Crystal-Structure Refinement and the Chemical Formula. *Crystals* **2025**, *15*, 799. https://doi.org/10.3390/cryst15090799

1. Introduction

Minerals containing rare earth elements (REEs) possess remarkable chemical and structural diversity with over 290 mineral species known today, which comprises about 4.8% of all known minerals. Recent discoveries [1–24] indicate that the research in REE descriptive mineralogy is very intense, owing to the importance of REEs in modern technology. Though the number of industrially interesting REE minerals is rather limited, investigations of the occurrence and crystal chemistry of rare species are essential, due to the relevant information on the speciation of REEs in natural systems and mechanisms of their incorporation into crystal structures of minerals. Last but not least in importance are the studies of REE minerals as prototypes of novel materials for various kinds of applications, especially those connected with green technologies. It is worth noting that not all REE minerals have synthetic analogs, so mineralogical discoveries may provide inspiration for the synthesis of new compounds with important properties [25].

Of special interest are REE minerals that contain heavy rare earths (HREEs), such as Dy, Er, Yb, etc. One of the mineral world localities where HREE minerals have been found is Ploskaya Mountain, located in the Keivy Massif, Kola Peninsula, Russia. In this locality, HREEs are incorporated into Y minerals of amazonitic pegmatites, sometimes forming their own mineral species such as xenotime-(Yb), $YbPO_4$ [26], hingganite-(Yb), $YbBe(SiO_4)(OH)$ [27], and keiviite-(Yb), $Yb_2Si_2O_7$ [28]. Mineralogy and geochemistry of the Ploskaya minerals have been studied by Voloshin and Pakhomovsky [29], who described some interesting REE minerals and, in particular, caysichite-(Y), which is a subject of the current study.

Caysichite-(Y) was reported as a new mineral species by Hogarth et al. [30] from granite pegmatites at the abandoned Enas-Lou feldspar mine, 22 miles north of Ottawa (Canada). The mineral was assigned the formula $(Y,Ca)_4Si_4O_{10}(CO_3)_3{\cdot}4H_2O$ and was described as orthorhombic, $Ccm2_1$ or $Ccmm$, a = 13.282, b = 13.925, c = 9.729 Å. It should be noted immediately that the charge-balance conditions require the amounts of Y and Ca atoms per formula unit (apfu) to be equal, which results in the electroneutral formula $Y_2Ca_2Si_4O_{10}(CO_3)_3{\cdot}4H_2O$. However, the Ca amount in Canadian caysichite-(Y) was essentially smaller than 2 (1.47 apfu), which raised the question of a possible charge-balance mechanism in its crystal structure. The latter was solved in 1978 on the Canadian material by Mellini and Merlino [31], who outlined basic structural features of the mineral, based upon double-crankshaft silicate chains, $[Si_4O_{10}]$, linked into a three-dimensional framework by MO_8 polyhedra (M = REEs, Ca) with carbonate groups, (CO_3), located in between the chains. The mineral was defined as orthorhombic, $Ccm2_1$ (a = 13.27(1), b = 13.91(1), c = 9.73(1) Å); the crystal structure was refined to R = 0.06 on the basis of 959 independent reflections. Mellini and Merlino [31] determined that the crystal structure contains two M sites, one fully occupied by Y, and the second occupied by Ca and unspecified 'rare-earth cation' with the ratio Ca:REE equal to 3:1. The total charge of the (Ca+REE) sum for 8 apfu was, therefore, defined as 21+, whereas the total negative charge of the anionic part ($2[Si_4O_{10}] + 6(CO_3)$) equals 20–. In order to compensate for the charge imbalance, it was assumed that one of the H_2O sites in the structure accommodates hydroxyl anions, $(OH)^-$. The formula of caysichite-(Y) proposed by Mellini and Merlino [31] was as follows: $Y_4(Ca_3REE_1)(OH)(H_2O)_5[Si_8O_{20}]{\cdot}2H_2O$. The chemical formula of the mineral currently accepted by the International Mineralogical Association (IMA) is $(Ca,Yb,Er)_4Y_4(Si_8O_{20})(CO_3)_6(OH){\cdot}7H_2O$ [32].

After the first description of caysichite-(Y) [30] and its structural determination [31] (the remark is in order that the first name of the mineral was 'caysichite', and it was later renamed as 'caysichite-(Y)', following the formal procedure of renaming all REE minerals [33] in accord with the Levinson nomenclature [34]); the mineral was reported from several

world localities, including Lindvikskollen Quarry, Telemark, Norway [35]; Suishoyama mine, Fukushima Prefecture, Japan [36]; Rio Stogia, Liguria, Italy [37]; Paratoo mine, South Australia [38]; Chudnoe Gold Deposit, Subpolar Ural, Russia [39]; Steinerleinbach Quarry, Bavaria, Germany [40]; and Malossa Mount, Malawi [41]. Voloshin et al. [42] described caysichite-(Y) from amazonitic pegmatites of the Ploskaya Mountain (Kola Peninsula, Russia), and this is the locality of origin of the sample studied herein.

The purpose of the current work is the crystal–chemical study of caysichite-(Y) from the Kola Peninsula in order to refine its structural parameters and to shed new light onto its chemical formula, which, in our opinion, has to be reconsidered after the study of material from different geological localities.

2. Materials and Methods

2.1. Materials

The sample of caysichite-(Y) used in this study originates from the Western Keivy Massif (Kola Peninsula, Russia) that contains peralkaline granite- and pegmatite-hosted REE deposits of different sizes and REE contents (Figure 1). The pegmatite with the samples of caysichite-(Y) and other REE minerals belongs to the Vyuntspakhk field that hosts 23 separate pegmatite veins [43]. The amazonite pegmatite vein at Mt. Ploskaya is located in biotite gneiss near its contact with peralkaline granite. The vein is ~210 m in length, and has an average thickness of 25 m. The vein is zoned, with an outer part composed of medium-grained quartz and albite, an intermediate zone of very coarse-grained amazonite, and a core of quartz and albite, including large monomineralic blocks of smoky quartz [43]. The Ploskaya locality was the source of an ornamental amazonite and was exploited in the 1970s and 1980s. The Ploskaya pegmatite contains an abundance of REE minerals, including Y-rich fluorite, vyuntspakhkite-(Y), hingganite-(Y), hingganite-(Yb), keiviite-(Y), keiviite-(Yb), kuliokite-(Y), fluorthalénite-(Y), monazite-(Ce), bastnäsite-(Ce), xenotime-(Y), churchite-(Y), zircon, pyrochlore, fergusonite-(Y), euxenite-(Y), and aeschynite-(Ce).

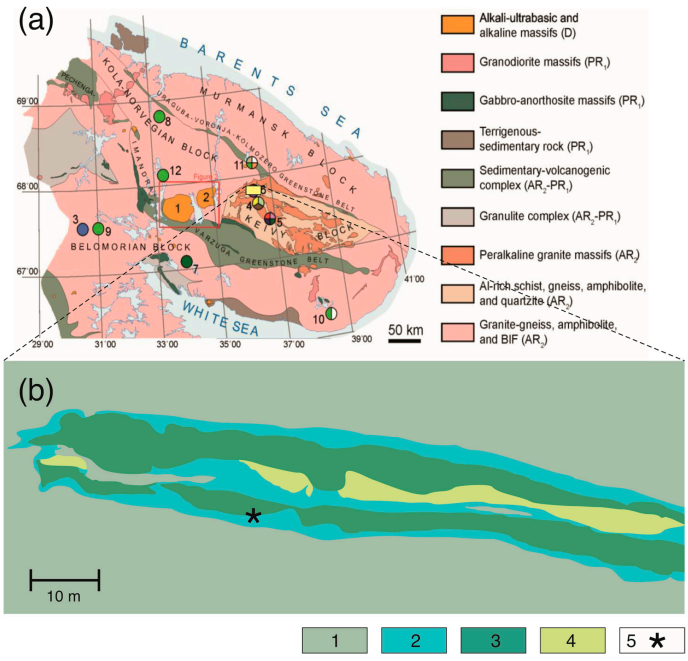

Figure 1. Geological map of the Kola Peninsula (modified after [43]) (**a**) and the scheme of the Mt. Ploskaya pegmatite (**b**); modified after [29]; legend: 1—Archaean biotite gneiss; 2—quartz–albite zone; 3—amazonite zone; 4—the zone of blocky quartz; 5 (*) —the place of the sample selection).

The crystals of caysichite-(Y) studied in this work were found in association with fluorite forming nests within albite and amazonite. Other associated minerals are thalénite, keivyite-(Y), xenotime-(Y), and kainosite-(Y). Caysichite-(Y) forms white spherolites of transparent needle-like crystals elongated along [001].

2.2. Chemical Composition

The elemental analysis of caysichite-(Y) was carried out using a scanning electron microscope LEO-1450 (Carl Zeiss Microscopy, Munich, Germany) equipped with an energy-dispersive spectrometer ULTIM MAX 100 (Oxford Instruments, Oxfordshire, UK), at an accelerating voltage of 20 kV and a probe current of 2 nA. The results are given in Table 1 in comparison with the analytical data for caysichite-(Y) from the previous studies. The energy-dispersive spectra were processed automatically using the AzTec Energy software package. The chemical formula was calculated based on Si + Al = 4; the data from the previous studies were recalculated on the same basis. The standards used for the microprobe work were synthetic $Y_3Al_5O_{12}$ (Y and Al), synthetic $LiREE(MoO_4)_2$ (REE = Yb, Er, Lu, Tm, Gd), $LiREE'(WO_4)_2$ (REE' = Dy and Ho), diopside (Ca and Si), and fluorite (F).

Table 1. Chemical composition (in apfu) of caysichite-(Y) * and calculated average site-scattering factor (<SSF>, e^-) of the M sites in its crystal structure.

	1 **	**2** **	**3**	**4**	**5**
Al	n.d. ***	n.d.	n.d.	n.d.	0.09
Si	4.00	4.00	4.00	4.00	3.91
Ca	1.87	1.52	1.43	1.28	1.46
Ba	0.01	n.d.	n.d.	n.d.	n.d.
Y	1.63	1.84	2.04	1.16	2.03
Tb	n.d.	n.d.	n.d.	n.d.	0.01
Ce	n.d.	n.d.	n.d.	n.d.	0.01
La	0.01	n.d.	n.d.	n.d.	n.d.
Pr	0.01	n.d.	n.d.	n.d.	n.d.
Nd	0.02	0.01	n.d.	n.d.	0.01
Sm	0.01	n.d.	n.d.	n.d.	0.01
Gd	0.02	0.01	0.01	n.d.	0.02
Dy	0.06	0.06	0.03	0.08	0.05
Ho	0.02	0.02	0.01	0.03	0.03
Er	0.09	0.10	0.06	0.22	0.08
Tm	0.02	0.03	0.01	0.07	0.01
Yb	0.13	0.16	0.12	0.80	0.09
Lu	0.02	0.02	0.02	0.10	0.02
(Ca+REE)	3.92	3.77	3.73	3.74	3.83
CO_3	2.95	2.89	2.89	2.99	2.99
H_2O	3.85 ****	3.85 ****	n.d.	n.d.	3.93
<SSF>	32.42	32.44	31.63	40.49	32.93

* **1**, **2** (used for the crystal-structure analysis)—this work; **3**, **4**—Voloshin et al. [42]; **5**—Hogarth et al. [30]. ** each analysis is the average of 5–10 measurement spots. *** n.d. = none detected; the detection limit is 0.1 wt.%. **** calculated on the basis of crystal-structure data.

2.3. Single-Crystal X-Ray Diffraction Analysis

The crystal-structure study of caysichite-(Y) was carried out by means of the Synergy S single-crystal diffractometer equipped with the Hypix detector at room temperature. The monochromatic Mo$K\alpha$ radiation (λ = 0.71069 Å) was used. More than half of the diffraction sphere was collected with a scanning step of 1° and an exposure time of 90 s. The data integration and correction was performed using the CrysAlis program package. The same package was used for the empirical absorption correction using spherical harmonics, implemented in the SCALE3 ABSPACK scaling algorithm [44]. The structure was refined using the SHELXTL 5.1 software package [45] in the $Ccm2_1$ space group (non-standard setting of the $Cmc2_1$ group used by Mellini and Merlino [31,46]), using the initial atom coordinates determined in [31]. The positions of H atoms could not be located. Crystal data, data collection information, and structure refinement details are given in Table 2; atom

coordinates and displacement parameters are in Table 3, and selected interatomic distances are in Table 4. Table 5 provides refined site-scattering factors for the two M sites occupied by REEs and Ca with proposed occupancies. It should be noted that the occupancies given in Table 5 should be considered as plausible hypotheses, since the exact assignment of different elements to the particular site cannot be performed at the current state of experimental technique and knowledge. Table 6 contains the results of bond–valence analysis performed using bond–valence parameters taken from [47].

Table 2. Crystal data and structure refinement for caysichite-(Y).

Crystal Data	
Chemical formula	$(Y_{1.84}Ca_{1.52}Yb_{0.16}Er_{0.10}Dy_{0.06}Tm_{0.03}Ho_{0.02}Lu_{0.02}Nd_{0.01}Gd_{0.01})_{3.77}[Si_4O_{10}](CO_3)_3(H_2O)_{3.85}$
M_r	407.62
Crystal system, space group	Orthorhombic, $Ccm2_1$ (no. 36)
Temperature (K)	296(2)
a, b, c (Å)	13.2693(3), 13.9455(4), 9.7384(2)
V (Å^3)	1802.06(8)
Z	4
μ (mm^{-1})	8.654
ρ (g/cm^3)	3.005
Crystal size (mm^3)	0.10 × 0.04 × 0.02
Data collection parameters	
Diffractometer	Rigaku XtaLAB Synergy-S
Radiation type	Mo$K\alpha$
Absorption correction	Gaussian
$2\Theta_{min}$, $2\Theta_{max}$	3.716, 37.135
No. of measured, independent and observed [$I > 2\sigma(I)$] reflections	26,875, 4472, 3906
R_{int}	0.045
Refinement parameters	
R_1 [$F^2 > 2\sigma(F^2)$], $wR(F^2)$, S	0.051, 0.107, 1.140
No. of reflections	4472
No. of parameters	167
$\Delta\rho_{max}$, $\Delta\rho_{min}$ (e Å^{-3})	2.030, −1.652

Table 3. Atomic coordinates and displacement parameters (Å^2) for caysichite-(Y).

Atom	Occupancy	x	y	z	U_{eq}
M1	see Table 5	0.14208(5)	0.16978(7)	0.04285(6)	0.0118(2)
M2	see Table 5	0.14500(6)	0.16844(9)	0.45700(7)	0.0157(2)
Si1	$Si_{1.00}$	0.40096(16)	−0.1111(2)	0.0902(3)	0.0088(4)
Si2	$Si_{1.00}$	0.40437(16)	0.1107(2)	0.4063(3)	0.0071(4)
O1	$O_{1.00}$	0.3721(8)	0	0.0620(12)	0.022(2)
O2	$O_{1.00}$	0.3702(7)	0	0.4340(10)	0.017(2)
O3	$O_{1.00}$	0.4394(3)	0.1225(3)	0.2430(8)	0.0153(7)
O4	$O_{1.00}$	0.3113(4)	0.1827(4)	0.0495(10)	0.015(1)
O5	$O_{1.00}$	0.3160(4)	0.1804(5)	0.4499(9)	0.016(1)
O6	$O_{1.00}$	0.4980(7)	0.1374(3)	−0.0026(9)	0.0216(8)
O7	$O_{1.00}$	0.1634(4)	0.1365(4)	0.752(2)	0.070(3)
O8	$O_{1.00}$	0.0235(6)	0.1599(5)	0.6384(8)	0.023(2)
O9	$O_{1.00}$	0.0212(6)	0.1642(6)	0.8677(9)	0.025(2)
O10	$O_{1.00}$	0.1432(6)	0	0.0572(9)	0.024(1)
O11	$O_{1.00}$	0.1717(3)	0.0810(3)	0.2504(9)	0.0178(7)
O12	$H_2O_{1.00}$	0.1507(3)	0.2776(3)	0.2471(11)	0.0207(7)
O13	$H_2O_{0.85}$	0.3456(13)	0	0.752(3)	0.079(5)
O14	$H_2O_{1.00}$	0.1706(9)	0	0.5276(13)	0.045(3)
C1	$C_{1.00}$	0.0690(4)	0.1526(4)	0.7611(10)	0.015(1)
C2	$C_{1.00}$	0.1629(6)	0	0.1852(9)	0.014(1)

Table 3. *Cont.*

Atom	U_{11}	U_{22}	U_{33}	U_{23}	U_{13}	U_{12}
M1	0.0078(3)	0.0134(3)	0.0142(4)	0.0023(4)	−0.0059(3)	−0.0017(3)
M2	0.0091(4)	0.0211(5)	0.0168(5)	−0.0049(5)	−0.0004(3)	−0.0020(3)
Si1	0.0098(8)	0.0093(10)	0.0071(8)	−0.0006(7)	0.0002(7)	−0.0001(7)
Si2	0.0052(7)	0.0065(9)	0.0097(9)	−0.0006(6)	−0.0010(6)	0.0020(6)
O1	0.028(4)	0.007(3)	0.031(6)	0	0.012(4)	0
O2	0.024(3)	0.007(3)	0.019(4)	0	0.020(3)	0
O3	0.0205(16)	0.0200(16)	0.0055(16)	−0.003(2)	−0.001(2)	−0.0029(12)
O4	0.0131(19)	0.010(2)	0.022(3)	0.010(3)	0.003(3)	0.0049(18)
O5	0.009(2)	0.019(3)	0.019(3)	0.001(3)	0.008(2)	0.005(2)
O6	0.0160(16)	0.0282(19)	0.0207(16)	0.006(3)	0.0109(13)	−0.001(4)
O7	0.012(2)	0.030(3)	0.167(9)	−0.014(10)	0.012(8)	0.0008(19)
O8	0.032(4)	0.023(3)	0.014(3)	−0.005(2)	0.011(3)	−0.005(3)
O9	0.023(3)	0.039(4)	0.013(3)	−0.001(3)	0.003(2)	−0.011(3)
O10	0.027(4)	0.023(3)	0.023(4)	0	−0.002(3)	0
O11	0.0252(17)	0.0124(14)	0.0157(15)	−0.003(3)	−0.006(3)	0.0015(13)
O12	0.0234(17)	0.0193(17)	0.0194(17)	0.009(3)	−0.001(3)	−0.0028(14)
O13	0.082(11)	0.081(10)	0.074(10)	0	−0.059(11)	0
O14	0.054(6)	0.021(4)	0.060(7)	0	0.035(6)	0
C1	0.0159(19)	0.017(2)	0.011(3)	0.000(2)	−0.001(2)	0.0002(15)
C2	0.012(3)	0.014(3)	0.015(3)	0	0.003(3)	0

Table 4. Selected interatomic distances (Å) for the crystal structure of caysichite-(Y).

M1–O4	2.254(6)	Si1–O3	1.582(8)
M1–O9	2.343(9)	Si1–O4	1.603(6)
M1–O5	2.344(8)	Si1–O6	1.615(9)
M1–O10	2.372(1)	Si1–O1	1.620(4)
M1–O8	2.390(9)	<Si1–O>	1.605
M1–O11	2.402(8)		
M1–O12	2.496(9)	Si2–O5	1.582(6)
M1–O7	2.89(2)	Si2–O6	1.614(9)
<M1–O>	2.436	Si2–O2	1.631(3)
		Si2–O3	1.665(8)
M2–O5	2.276(6)	<Si2–O>	1.623
M2–O4	2.336(6)		
M2–O9	2.371(8)	C1–O7	1.276(7)
M2–O11	2.379(8)	C1–O8	1.343(13)
M2–O8	2.394(8)	C1–O9	1.227(12)
M2–O14	2.471(5)	<C1–O>	1.282
M2–O12	2.550(8)		
M2–O7	2.91(2)	C2–O10	1.273(12)
<M2–O>	2.461	C2–O11	1.301(7) 2×
		<C2–O>	1.292

Table 5. Site-scattering factors and site occupancies for the M sites in the crystal structure of caysichite-(Y).

Site	SSF_{exp} [e^-]	Occupancy	SSF_{calc} [e^-]
		Analysis **1**	
M1	33.54	$Y_{0.41}Ca_{0.46}Er_{0.12}\square_{0.01}$	33.35
M2	31.98	$Y_{0.41}Ca_{0.46}Er_{0.10}\square_{0.03}$	31.99
		Analysis **2**	
M1	33.54	$Y_{0.47}Ca_{0.35}Er_{0.12}\square_{0.06}$	33.49
M2	31.98	$Y_{0.47}Ca_{0.41}Er_{0.08}\square_{0.04}$	31.97

Table 6. Bond–valence analysis (valence units = v.u.) for the crystal structure of caysichite-(Y).

Site	O1	O2	O3	O4	O5	O6	O7	O8	O9	O10	O11	O12	O14	Σ
							M = Y							
M1				0.51	0.41		0.11	0.36	0.41	0.38	0.35	0.28		2.81
M2				0.41	0.48		0.10	0.36	0.38		0.37	0.25	$0.30^{2\times\downarrow}$	2.65
Si1	$1.01^{2\times\downarrow}$		1.11	1.06		1.02								4.20
Si2		$0.98^{2\times\downarrow}$	0.90		1.11	1.03								4.02
C1							1.36	1.15	1.54					4.05
C2										1.37	$1.28^{2\times\rightarrow}$			3.93
Σ	2.02	1.96	2.01	1.98	2.00	2.05	1.57	1.87	2.33	1.75	2.00	0.53	0.60	
							M = Ca							
M1				0.43	0.34		0.09	0.31	0.34	0.32	0.30	0.24		2.37
M2				0.35	0.41		0.09	0.3	0.32		0.32	0.21	$0.25^{2\times\downarrow}$	2.25
Si1	$1.01^{2\times\downarrow}$		1.11	1.06		1.02								4.20
Si2		$0.98^{2\times\downarrow}$	0.90		1.11	1.03								4.02
C1							1.36	1.15	1.54					4.05
C2										1.37	$1.28^{2\times\rightarrow}$			3.93
Σ	2.02	1.96	2.01	1.84	1.86	2.05	1.54	1.76	2.20	1.69	1.90	0.45	0.50	

3. Results

3.1. Cation Coordination and Site Occupancies

The crystal structure of caysichite-(Y) contains two sites occupied by REEs and Ca (Figure 2). The coordination of both sites is eightfold and can be described as bicapped trigonal prismatic. The central prisms for the $M1O_8$ and $M2O_8$ polyhedra are formed by the O4, O5, O8, O9, O10, and O12 atoms, whereas additional M–O bonds are to the O7 and O11 atoms. The M1–O7 and M2–O7 bonds are the longest M–O bonds (2.89 and 2.91 Å, respectively).

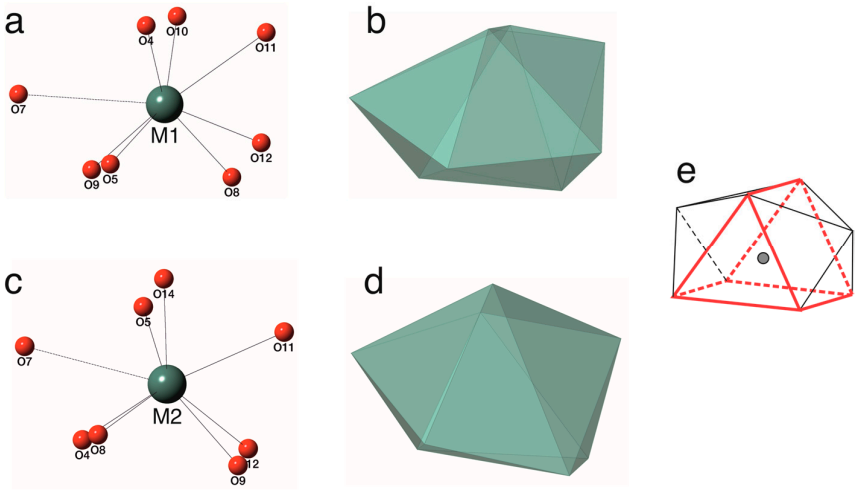

Figure 2. Coordination environments of the M1 (**a**,**b**) and M2 (**c**,**d**) sites shown in ball-and-stick and polyhedral representations, in comparison with an idealized version of a bicapped trigonal prism (**e**). Legend: M atoms and polyhedra are shown in green; O atoms are shown as red spheres; in (**e**), red lines outline contour of the central trigonal prism; in (**a**) and (**c**), the M–O bonds longer than 2.8 Å are shown as dashed lines.

The refinement of the M1 and M2 site occupancies indicated that their site-scattering factors (SSFs) are very similar (Table 5), differing by *ca.* 1.5 e^- only. The average <SSF> for the M sites obtained from the crystal-structure analysis (32.76 e^-) is in good agreement with the <SSF> value calculated using the empirical chemical formula (32.44 e^-; see Table 1). The proposed occupancies of the M sites are given in Table 5 (for the analyses **1** and **2** given in

Table 1), where Er is taken as the average representative of lanthanides. As can be seen, for both sites, REEs predominate over Ca. Therefore, according to the IMA dominant-valency rule [48,49], our caysichite-(Y) should be considered as REE^{3+}-dominant species, that is, as a Y-dominant mineral. The M2 site contains more Ca, which agrees well with the average <M2-O> distance of 2.461 Å, which is somewhat longer than that for the M1 site (2.436 Å). The Ca^{2+}, Y^{3+}, and Er^{3+} cation radii for the [8]-coordination are 1.132, 1.024, and 0.998 Å [50], which supports the proposed site occupancies (Table 5). The proposed site occupancies are also supported by the results of bond–valence analysis (Table 6). The bond–valence sums of the M1 and M2 sites calculated using the Y–O bond–valence parameters are 2.81 and 2.65 v.u., whereas the same values calculated using the Ca-O parameters are 2.37 and 2.25 v.u., which supports the conclusion that the M2 site incorporates more Ca^{2+} cations than the M1 site.

In their crystal-structure refinement of caysichite-(Y), Mellini and Merlino [31] stated that the M1 site (the 'Y' site in their nomenclature) is fully occupied by Y, whereas the M2 site (or the 'CaRE' site) 'is occupied by calcium and rare-earth cations with an estimated ratio Ca:RE = 3:1' [31]. Taking into account the average <SSF> value of 32.93 e^- for the M sites calculated for the Canadian material from the data of Hogarth et al. [30] (Table 1), the SSF values for the M1 and M2 sites determined by Mellini and Merlino [31] are 39 and 26.86 e^-, respectively. These values are essentially different from those observed in our study and indicate the predominance of Ca in the M2 site. The average <M1-O> and <M2-O> distances for the Canadian caysichite-(Y) are 2.403 and 2.492 Å, respectively, which also differ from those for the Kola material. It should be noted that Mellini and Merlino [31] assumed full occupancies of the M1 and M2 sites, despite the fact that the chemical analyses indicate the average (REE+Ca) sum equal to 3.83. As will be shown below, the discrepancy from the ideal value of 4.00 may be essential for maintaining the electroneutrality of the crystal structure.

The inspection of the chemical analyses of caysichite-(Y) given in Table 1 shows that the amount of HREEs (in particular, ytterbium) in the mineral may be quite high (analysis **4**) and, in fact, may lead to the predominance of Yb over Y in one of the M sites (most probably, in the M1 site). Thus, analysis **4** may actually belong to a separate mineral species, 'caysichite-(Yb)', which requires detailed characterization of its composition, structure, and properties.

In agreement with the results reported in [31], there are two Si and two C sites in the crystal structure of caysichite-(Y), which demonstrate typical bond–length and bond–valence variations for silicates and carbonates (Tables 4 and 6). It is important to note that the Si sites in the Canadian material contain 0.09 apfu of Al (for Si+Al = 4), whereas the studied Kola samples have no Al in their composition.

3.2. Structure Description

The main features of the structural organization of caysichite-(Y) have been established in [31]. The crystal structure of the mineral is based upon a three-dimensional framework formed by chains of MO_8 polyhedra and SiO_4 tetrahedra (Figure 3a). The silicate units are double-crankshaft chains (Figure 3b,d) that serve as basic building units for a number of tetrahedral structures, including aluminosilicates of the feldspar group and zeolites [51–53]. As another basic building unit for caysichite-(Y), Mellini and Merlino [31] suggested considering double chains of MO_8 polyhedra running along [001] with their planes oriented parallel to (110) and $(1\bar{1}0)$. Herein, we adopt another approach to the description of the structure based upon the columns of MO_8 polyhedra and (CO_3) groups shown in Figure 3b,e and centered at the [00*z*]-axis. The mode of linkage of these chains to the crankshaft silicate chains is demonstrated in Figure 3f. In order to provide a clearer

view of the structural topology of caysichite-(Y), we use a nodal representation widely exploited in modern structural mineralogy and crystal chemistry [54].

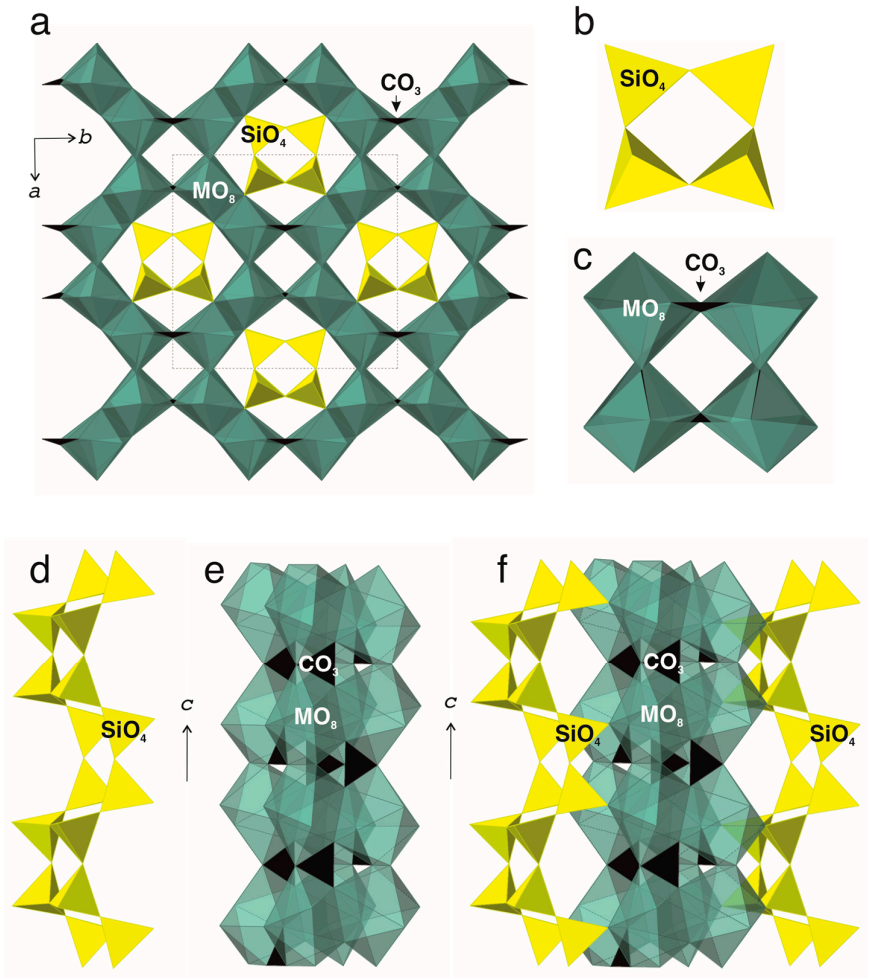

Figure 3. The crystal structure of caysichite-(Y) projected along the *c*-axis (**a**); projections of the crankshaft silicate chain (**b**) and the column of MO_8 polyhedra and (CO_3) groups (**c**) along the *c*-axis; the crankshaft silicate chains (**d**) and the columns (**e**) in peripheral view; the linkage mode between the chains and columns (**f**). Legend: MO_8, SiO_4, and CO_3 polyhedra are shown in dark green, yellow, and black, respectively.

Figure 4a,b shows the silicate crankshaft chain in caysichite-(Y) in polyhedral and ball-and-stick representations, respectively. In the nodal representation, Si nodes are linked by single lines (Figure 4c) if corresponding silicate tetrahedra share common corners. All atoms and bonds except Si atoms and Si–Si links are eliminated; the resulting graph characterizes the topology of linkage of SiO_4 tetrahedra within the chain (Figure 4d). The same procedure applied to the MO_8-CO_3 columns (Figure 4e–g) with M–M links shorter than 5 Å results in the graph describing the topology of linkage of MO_8 polyhedra (Figure 4h). It is remarkable that the M chain graph has the same topology as the Si chain, i.e., the topology of a double-crankshaft silicate chain. Figure 5a shows the crystal structure of caysichite-(Y) as composed from M and Si graphs with the M–M and Si–Si links shorter than 5 and 3.5 Å, respectively. The double M chains are linked by additional M–M edges into a three-dimensional framework with the **pcl** topology observed in paracelsian and structurally related phases [52]. The ideal symmetry for the **pcl** topology is *Cmcm* (no. 63), which is a minimal non-isomorphic supergroup for the space group $Ccm2_1$ (no. 36) found for caysichite-(Y).

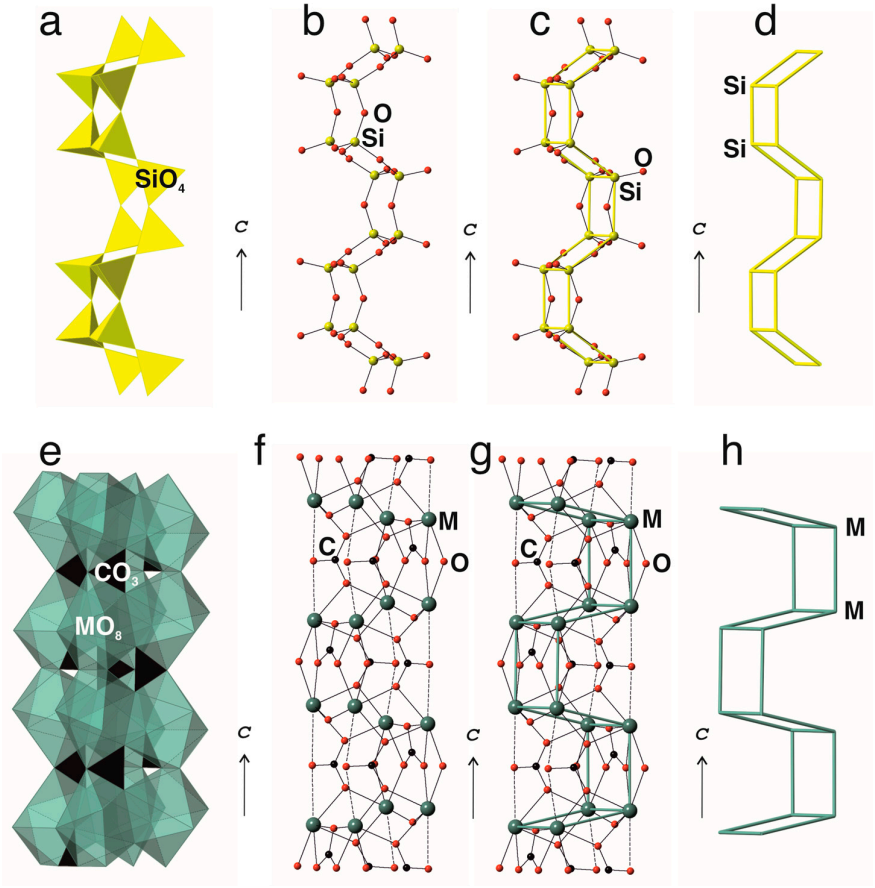

Figure 4. The double-crankshaft silicate chain in caysichite-(Y): polyhedral view (**a**), ball-and-stick view (**b**), ball-and-stick view with Si–Si links (**c**), and Si graph (**d**). The column of MO_8 polyhedra and (CO_3) groups: polyhedral view (**e**), ball-and-stick view (**f**), ball-and-stick view with M–M links (**g**), and M graph (**h**). Legend: MO_8, SiO_4, and CO_3 polyhedra are shown in dark green, yellow, and black, respectively; C, O, Si, and M atoms are shown as black, red, yellow, and dark-green spheres, respectively.

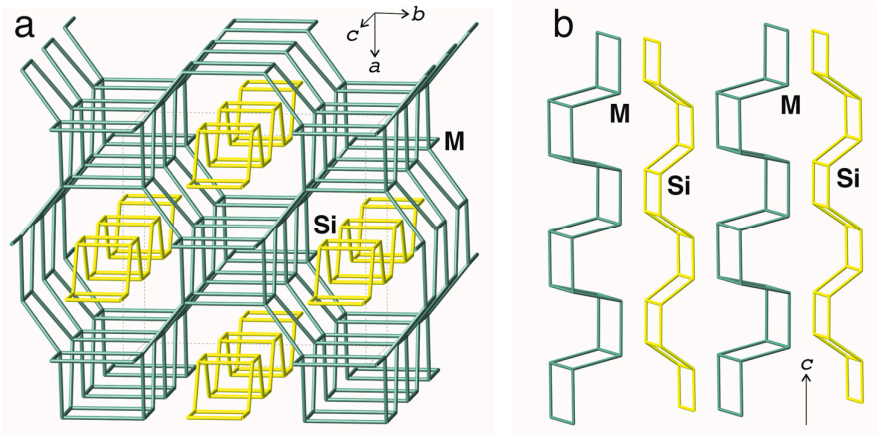

Figure 5. The crystal structure of caysichite-(Y) consists of M and Si graphs (**a**) and the relations between double-crankshaft M and Si chains (**b**).

The **pcl**-type M network in caysichite-(Y) contains large channels that accommodate double-crankshaft Si chains. The relations between the M and Si chains are shown in Figure 5b. The fourfold rings of both chains oriented along the *c*-axis are parallel and are in correspondence to each other, though the dimensions of the M_4 ring (~4.0 × 4.7 Å^2) are larger than those of the Si_4 rings (~3.1 × 3.1 Å^2).

3.3. Anion Sites and Hydrogen Bonding

As mentioned above, the efforts to localize and refine the positions of the H atoms have met no success. Therefore, the hydrogen bonding scheme can be described based on the anion–anion distances only.

In agreement with the general proposal by Mellini and Merlino [31], the O12, O13, and O14 sites have been assigned to H_2O molecules. The O12 and O14 sites are bonded to two M sites each, with the bond–valence sums equal to 0.45–0.60 v.u. (Table 6), depending upon the bond–valence parameters used. These bond–valence sums agree well with the occupation of these sites by H_2O molecules. The bond–valence sums calculated for the O12 and O14 sites in [31] are 0.56 and 0.62 v.u., respectively. Mellini and Merlino [31] suggested that the O14 site is occupied by a hydroxyl ion and an H_2O molecule in the ratio $OH:H_2O = 1:1$. However, this scheme seems unlikely, since the bond–valence sum is rather low for this site to incorporate $(OH)^-$ ions. This proposal is also not supported from the viewpoint of chemical composition, as will be discussed below.

The inspection of the bond–valence sums for anions given in Table 5 shows that the bond–valence sum for the O7 site is relatively low (1.54 or 1.57 v.u.), which was also observed for the Canadian material (1.58 v.u.) [31]. The local environment of the O7 site in the crystal structure of caysichite-(Y) studied in this work is shown in Figure 6a. It forms two contacts to adjacent O12 and O14 sites occupied by H_2O molecules; the O···O distances and configuration of O atoms indicate that these contacts correspond to hydrogen bonds donated by H_2O molecules. Since the average bond valence of the H_2O···O bonds is 0.20 v.u., the total bond–valence sum for the O7 site is about 1.94 or 1.97 v.u., which is in good agreement with its assignment to an O^{2-} ion.

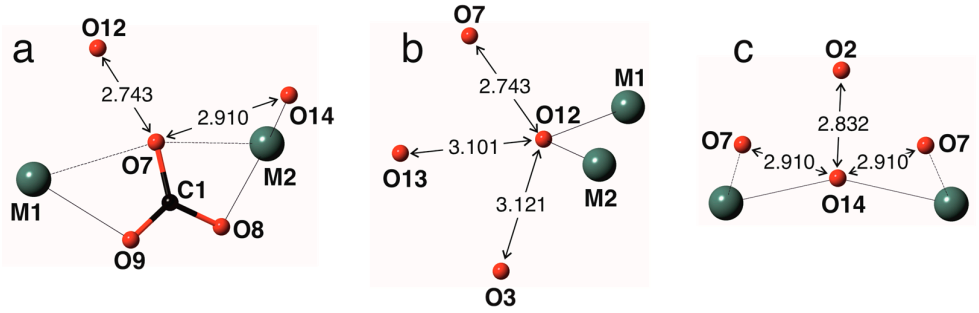

Figure 6. Local environments of the O7 (**a**), O12 (**b**), and O14 (**c**) sites in the crystal structure of caysichite-(Y).

Figure 6b,c shows local environments of the O12 and O14 sites occupied by H_2O molecules with the O···O distances that may be responsible for the formation of hydrogen bonds.

The O13 atom has no neighbors within the 3 Å sphere that would be indicative of any bonding, including hydrogen bonds. Thus, it is held in the structure rather loosely, which is also manifested in its relatively large displacement parameters compared to other anions (Table 3). The refined occupancy factor for this site is 0.85. It should be noted that the occupancy of the O13 site was not refined (or reported to be refined) by Mellini and Merlino [31], despite the large displacement parameters. Taking into account that the H_2O amount measured by Hogarth et al. [30] for the Canadian sample is 3.93, it seems reasonable to suggest that the O13 site in Canadian caysichite-(Y) may be under-populated as well.

4. Discussion

It has been mentioned above that the results of this study, in general, agree with the results of the crystal-structure solution and refinement of caysichite-(Y) undertaken by Mellini and Merlino [31]. However, there are some discrepancies that are of critical importance for the correct determination of crystal–chemical and ideal chemical formulas for this mineral.

1. Let us consider the anionic part of the crystal structure composed of the $[Si_4O_{10}]^{4-}$ double-crankshaft chains and $(CO_3)^{2-}$ carbonate groups. The total negative charge of the $\{[Si_4O_{10}](CO_3)_3\}$ part is 10– that has to be compensated by cations. The chemical study of our sample indicates that the cation content is $\{[REE^{3+}_{2.24}Ca^{2+}_{1.52}]_{3.76}\}^{9.77+}$, where Y^{3+} predominates over other rare earth cations. Thus, the total charge of the cationic part is 9.77+, which is less than required to compensate for the negative charge of the anionic part. The population analysis given in Table 5 shows that the M sites contain some vacancies (0.04–0.06 apfu). If both M1 and M2 sites are empty, the bond–valence sum incident upon the O7 site is 1.36 v.u., which is more typical for an $(OH)^-$ group than for an O^{2-} anion. Therefore, the minor protonation of the O7 atom belonging to the $C1O_3$ group may be considered as a possible mechanism of charge compensation in caysichite-(Y). Within this approach, the incorporation of hydroxyl ions into the H_2O sites (O12 or O14) as suggested in [31] is not needed;

2. The inspection of the chemical analyses of caysichite-(Y) given in Table 1 shows that the (REE+Ca) sum is always smaller than 4.00, required by the full occupancies of both M1 and M2 sites. This may indicate the importance of vacancies in the M sites in order to keep the crystal structure electroneutral. Both full occupancies and electroneutrality are observed only if the REE^{3+} and Ca^{2+} amounts are equal, that is, if the cation content is $\{[REE^{3+}_2Ca^{2+}_2]_4\}^{10+}$. This would correspond to the ideal formula of caysichite-(Y) written as $Y_2Ca_2[Si_4O_{10}](CO_3)_3 \cdot 4H_2O$. Under the condition of full occupancies of the M sites, the prevalence of REE over Ca would correspond to the total positive charge exceeding 10+ and the need for additional anionic species. This situation forced Mellini and Merlino [31] to assume incorporation of $(OH)^-$ groups into H_2O sites, which is rather unlikely, taking into account the results of the bond–valence analysis. However, the chemical formula of caysichite-(Y) reported by Hogarth et al. [30] has the total (REE+Ca) sum equal to 3.83, i.e., smaller than 4.00. The total positive charge of the (REE^{3+}+Ca^{2+}) sum in the Canadian sample is 10.07+, that is, higher than 10+ required for the structure electroneutrality. However, the Canadian caysichite-(Y) has 0.09 apfu of Al that lowers the negative charge of the anionic part from 10– to 9.91–. Again, in this case, there is also no need for the incorporation of hydroxyl into the H_2O sites. In order to account for the charge of the whole content of the M sites to be 10+ and taking into account the presence of vacancies, the M site content can be expressed as $[REE_{2+2x}Ca_{2-3x}\square_x]^{10+}$. For the Canadian sample, x = 0.17, and the cationic part should have the formula $[REE_{2.34}Ca_{1.49}\square_{0.17}]^{10+}$, which agrees well with the experimental content $[REE_{2.37}Ca_{1.46}\square_{0.17}]^{10.07+}$ (it should be noted that Canadian caysichite-(Y) contains some Ce^{4+}). For our sample (analysis **2** in Table 1), x = 0.23, theoretical M content is $[REE_{2.46}Ca_{1.31}\square_{0.23}]^{10+}$, whereas the experimental content is $[REE_{2.26}Ca_{1.52}\square_{0.23}]^{9.77+}$, which requires protonation of carbonate groups to maintain the electroneutrality;

3. The nature of predominant cations in the M sites is critical for the correct chemical formula of caysichite-(Y). In our case, Y predominates in both M sites, whereas Mellini and Merlino [31] indicated that, in the Canadian sample, the predominant elements in the M1 and M2 sites are Y and Ca, respectively. If this is the case, the mineral studied by us and caysichite-(Y) found in Canada and studied in [30,31] are different mineral species. However, we believe that there is a need for the additional investigation of the Canadian

material, since the excellent study by Mellini and Merlino [31] was performed slightly less than fifty years ago, and the quality of structure refinement may be improved (for instance, the refinement performed in [31] was based upon 959 reflections, whereas ours is based upon 4472 independent reflections). The high-precision refinement of Canadian caysichite-(Y) may provide additional data on the site-scattering factors of the M sites, which would shed new light upon the critical problem of the crystal–chemical identity of caysichite-(Y).

5. Conclusions

The crystal–chemical study of caysichite-(Y) from the Ploskaya Mt (Kola Peninsula, Russia) and its comparison with the previous data on the Canadian sample allows us to propose a new very general chemical formula of the potential caysichite-type mineral that may be written as $[REE_{2+2x-y'}Ca_{2-3x-y''}\square_{x+y'+y''}][Si_4O_{10}](HCO_3)_{3y'+2y''}(CO_3)_{3-3y'-2y''}\cdot(4-z)H_2O$, where $z \sim 0.2$; $x \leq 2/3$; $y' \leq 2/3$; $y'' \leq 1$; $3y'+2y'' \leq 2$. This general formula allows for several end-member formulas according to different x, y′, and y″ values and M-dominant REE (dREE):

(1) $x = y' = y'' = z = 0$; dREE = Y. The end-member formula is $(Y_2Ca_2)[Si_4O_{10}](CO_3)_3\cdot 4H_2O$;

(2) $x = y' = z = 0$; $y'' = 1$; dREE = Y. The end-member formula is $(Y_2Ca\square)[Si_4O_{10}](HCO_3)_2(CO_3)\cdot 4H_2O$;

(3) $y' = y'' = z = 0$; $x = 2/3$; dREE = Y. The end-member formula is $(Y_{10/3}\square_{2/3})[Si_4O_{10}](CO_3)_3\cdot 4H_2O$;

(4) $x = y'' = z = 0$; $y' = 2/3$; dREE = Y. The end-member formula is $(Ca_2Y_{4/3}\square_{2/3})[Si_4O_{10}](HCO_3)_2(CO_3)\cdot 4H_2O$.

For the two analyses (**1** and **2** in Table 1) reported in this work, the general formulae can be written as $(REE_{2.05}Ca_{1.87}\square_{0.18})[Si_4O_{10}](HCO_3)_{0.11}(CO_3)_{2.89}\cdot 3.8H_2O$ and $(REE_{2.25}Ca_{1.52}\square_{0.23})[Si_4O_{10}](HCO_3)_{0.21}(CO_3)_{2.79}\cdot 3.8H_2O$, respectively. The formulae can be obtained using the (x, y′, y″) sets of values equal to (0.025, 0, 0.055) and (0.125, 0, 0.115), respectively. The end-member formula most close to these compositions is $(Y_2Ca_2)[Si_4O_{10}](CO_3)_3\cdot 4H_2O$. The same formula is valid for other analyses given in Table 1, but it is different from the formula $(Ca,Yb,Er)_4Y_4(Si_8O_{20})(CO_3)_6(OH)\cdot 7H_2O$ adopted by the IMA and proposed by Mellini and Merlino [31], but more close (or generally identical) to the formula $(Y,Ca)_4Si_4O_{10}(CO_3)_3\cdot 4H_2O$ proposed in the original study of Hogarth et al. [30]. In order to resolve the problem of the caysichite-(Y) formula, additional studies of materials from different localities (and, especially, one from the holotype locality) are needed.

Author Contributions: Conceptualization, S.V.K. and V.N.Y.; methodology, S.V.K., O.F.G. and Y.A.P.; validation, S.V.K.; formal analysis, S.V.K., O.F.G. and Y.A.P.; investigation, S.V.K., V.N.Y., O.F.G. and Y.A.P.; data curation, S.V.K.; writing—original draft preparation, S.V.K.; writing—review and editing, V.N.Y.; visualization, S.V.K. and Y.A.P.; supervision, S.V.K.; project administration, S.V.K.; funding acquisition, S.V.K. All authors have read and agreed to the published version of the manuscript.

Funding: This research was funded in the framework of the state tasks FMEZ-2025-0070 (Nanomaterials Research Centre) and FMEZ-2024-0008 (Geological Institute) of the Kola Science Centre, Russian Academy of Sciences.

Data Availability Statement: The crystal structure data for caysichite-(Y) are available as a CIF file from the CCDC/FIZ Karlsruhe database as CSD # 2482225 at https://www.ccdc.cam.ac.uk (accessed on 7 September 2025).

Acknowledgments: The X–ray diffraction and chemical analytical studies were performed in the FRC KSC RAS Centre for Collective Use of Equipment.

Conflicts of Interest: The authors declare no conflicts of interest.

References

1. Campostrini, I.; Demartin, F.; Finello, G.; Vignola, P. Aluminotaipingite-(CeCa), $(Ce_6Ca_3)Al(SiO_4)_3[SiO_3(OH)]_4F_3$, a New Member of the Cerite-Supergroup Minerals. *Mineral. Mag.* **2023**, *87*, 741–747. [CrossRef]
2. Holtstam, D.; Casey, P.; Bindi, L.; Förster, H.-J.; Karlsson, A.; Appelt, O. Fluorbritholite-(Nd), $Ca_2Nd_3(SiO_4)_3F$, a New and Key Mineral for Neodymium Sequestration in REE Skarns. *Mineral. Mag.* **2023**, *87*, 731–737. [CrossRef]
3. Kampf, A.R.; Ma, C.; Marty, J. Chinleite-(Nd), $NaNd(SO_4)_2(H_2O)$, The Nd analogue of chinleite-(Y) from the Markey Mine, Red Canyon, San Juan County, Utah, Usa. *Can. J. Mineral. Petrol.* **2023**, *61*, 411–418. [CrossRef]
4. Liu, P.; Gu, X.; Zhang, W.; Hu, H.; Chen, X.; Wang, X.; Song, W.; Yu, M.; Cook, N.J. Jingwenite-(Y) from the Yushui Cu Deposit, South China: The First Occurrence of a V-HREE-Bearing Silicate Mineral. *Am. Mineral.* **2023**, *108*, 192–196. [CrossRef]
5. Lykova, I.; Rowe, R.; Poirier, G.; Friis, H.; Helwig, K. Mckelveyite Group Minerals Part 2: Alicewilsonite-(YCe), $Na_2Sr_2YCe(CO_3)_6{\cdot}3H_2O$, a New Species. *Eur. J. Mineral.* **2023**, *35*, 143–155. [CrossRef]
6. Ondrejka, M.; Uher, P.; Ferenc, Š.; Majzlan, J.; Pollok, K.; Mikuš, T.; Milovská, S.; Molnárová, A.; Škoda, R.; Kopáčik, R.; et al. Monazite-(Gd), a New Gd-Dominant Mineral of the Monazite Group from the Zimná Voda REE-U-Au Quartz Vein, Prakovce, Western Carpathians, Slovakia. *Mineral. Mag.* **2023**, *87*, 568–574. [CrossRef]
7. Števko, M.; Myšľan, P.; Biagioni, C.; Mauro, D.; Mikuš, T. Ferriandrosite-(Ce), a New Member of the Epidote Supergroup from Betliar, Slovakia. *Mineral. Mag.* **2023**, *87*, 887–895. [CrossRef]
8. Wang, Y.; Gu, X.; Dong, G.; Hou, Z.; Nestola, F.; Yang, Z.; Fan, G.; Wang, Y.; Qu, K. Calcioancylite-(La), $(La,Ca)_2(CO_3)_2(OH,H_2O)_2$, a New Member of the Ancylite Group from Gejiu Nepheline Syenite, Yunnan Province, China. *Mineral. Mag.* **2023**, *87*, 554–560. [CrossRef]
9. Wu, B.; Gu, X.-P.; Rao, C.; Wang, R.-C.; Xing, X.-Q.; Wan, J.-J.; Zhong, F.-J.; Bonnetti, C. Gysinite-(La), $PbLa(CO_3)_2(OH)H_2O$, a New Rare Earth Mineral of the Ancylite Group from the Saima Alkaline Complex, Liaoning Province, China. *Mineral. Mag.* **2023**, *87*, 143–150. [CrossRef]
10. Kasatkin, A.V.; Zubkova, N.V.; Škoda, R.; Pekov, I.V.; Agakhanov, A.A.; Gurzhiy, V.V.; Ksenofontov, D.A.; Belakovskiy, D.I.; Kuznetsov, A.M. The Mineralogy of the Historical Mochalin Log REE Deposit, South Urals, Russia. Part V. Zilbermintsite-(La), $(CaLa_5)(Fe^{3+}Al_3Fe^{2+})[Si_2O_7][SiO_4]_5O(OH)_3$, a New Mineral with ET2 Type Structure and a Definition of the Radekškodaite Group. *Mineral. Mag.* **2024**, *88*, 302–311. [CrossRef]
11. Liu, P.; Li, G.; Sun, N.; Yao, W.; Yu, H.; Tian, Y.; Yang, W.; Zhao, F.; Cook, N.J. Wenlanzhangite–(Y) from the Yushui Deposit, South China: A Potential Proxy for Tracing the Redox State of Ore Formation. *Am. Mineral.* **2024**, *109*, 1738–1747. [CrossRef]
12. Lykova, I.; Rowe, R.; Poirier, G.; Friis, H.; Helwig, K. Mckelveyite Group Minerals—Part 3: Bainbridgeite-(YCe), $Na_2Ba_2YCe(CO_3)6{\cdot}3H_2O$, a New Species from Mont Saint-Hilaire, Canada. *Eur. J. Mineral.* **2024**, *36*, 183–194. [CrossRef]
13. Lykova, I.; Rowe, R.; Poirier, G.; Friis, H.; Helwig, K. Mckelveyite Group Minerals—Part 4: Alicewilsonite-(YLa), $Na_2Sr_2YLa(CO_3)_6{\cdot}3H_2O$, a New Lanthanum-Dominant Species from the Paratoo Mine, Australia. *Eur. J. Miner.* **2024**, *36*, 301–310. [CrossRef]
14. Ondrejka, M.; Bačík, P.; Majzlan, J.; Uher, P.; Ferenc, Š.; Mikuš, T.; Števko, M.; Čaplovičová, M.; Milovská, S.; Molnárová, A.; et al. Xenotime-(Gd), a New Gd-Dominant Mineral of the Xenotime Group from the Zimná Voda REE-U-Au Quartz Vein, Prakovce, Western Carpathians, Slovakia. *Mineral. Mag.* **2024**, *88*, 613–622. [CrossRef]
15. Pekov, I.V.; Zubkova, N.V.; Kasatkin, A.V.; Chukanov, N.V.; Koshlyakova, N.N.; Ksenofontov, D.A.; Škoda, R.; Britvin, S.N.; Kirillov, A.S.; Zaitsev, A.N.; et al. Hydroxylbastnäsite-(La), an "Old New" Bastnäsite-Group Mineral. *Mineral. Mag.* **2024**, *88*, 755–765. [CrossRef]
16. Pieczka, A.; Kristiansen, R.; Stachowicz, M.; Dumanska-Slowik, M.; Goleebiowska, B.; Seęk, M.P.; Nejbert, K.; Kotowski, J.; Marciniak-Maliszewska, B.; Szuszkiewicz, A.; et al. Heflikite, Ideally $Ca_2(Al_2Sc)(Si_2O_7)(SiO_4)O(OH)$, the First Scandium Epidote-Supergroup Mineral from Jordanów Śląeski, Lower Silesia, Poland and from Heftetjern, Tordal, Norway. *Mineral. Mag.* **2024**, *88*, 228–243. [CrossRef]
17. She, H.; Liu, S.; Fan, H.; Gu, X.; Li, X.; Yang, K.; Wang, Q. Oboniobite and Scandio-fluoro-eckermannite, Two New Minerals in the Bayan Obo Deposit, Inner Mongolia. *Chin. J. Geol.* **2024**, *59*, 1466–1469. [CrossRef]
18. Yang, J.; Du, W. High-Pressure Minerals and New Lunar Mineral Changesite-(Y) in Chang'e-5 Regolith. *Matter Radiat. Extrem.* **2024**, *9*, 027401. [CrossRef]
19. Yao, W.; Liu, P.; Li, G.; Sun, N.; Yang, W.; Jiang, C.; Du, W.; Zhang, C.; Song, W.; Cook, N.J.; et al. Yuchuanite-(Y), $Y_2(CO_3)_3{\cdot}H_2O$, a New Hydrous Yttrium Carbonate Mineral from the Yushui Cu Deposit, South China. *Am. Mineral.* **2024**, *109*, 599–605. [CrossRef]
20. Zhu, Z.; Wang, D.; Yu, H.; Chen, Z.; Li, Y.; Li, J.; Ren, J. Discovery and Geological Significance of New Mineral Tantalaeschynite-(Ce). *Geol. Surv. China* **2024**, *11*, 1–10. [CrossRef]
21. Kampf, A.R.; Ma, C.; Marty, J. Chinleite-(Ce), $NaCe(SO_4)_2(H_2O)$, a new mineral from the Blue Streak Mine, Montrose County, Colorado, USA. *Can. J. Mineral. Petrol.* **2025**, *63*, 199–204. [CrossRef]

22. Malcherek, T.; Schlüter, J.; Husdal, T. Anorthoyttrialite-(Y), $Y_4(SiO_4)(Si_3O_{10})$, a Natural Representative of B-Type Rare Earth Disilicates. *Mineral. Mag.* **2025**, *89*, 428–442. [CrossRef]
23. Plášil, J.; Steciuk, G.; Sejkora, J.; Kampf, A.R.; Uher, P.; Ondrejka, M.; Škoda, R.; Dolníček, Z.; Philippo, S.; Guennou, M.; et al. Extending the mineralogy of U^{6+}. I. Crystal structure of lepersonnite-(Gd) and a description of the new mineral lepersonnite-(Nd). *Mineral. Mag.* **2025**, *in press*. [CrossRef]
24. Plášil, J.; Steciuk, G.; Škoda, R.; Philippo, S.; Guennou, M. Extending the mineralogy of U^{6+}. III. Pendevilleite-(Y), a new uranyl carbonate mineral from Kamoto-East Open-Cut, Democratic Republic of Congo. *Mineral. Mag.* **2025**, *in press*. [CrossRef]
25. Bindi, L.; Nespolo, M.; Krivovichev, S.V.; Chapuis, G.; Biagioni, C. Producing Highly Complicated Materials. Nature Does It Better. *Rep. Prog. Phys.* **2020**, *83*, 106501. [CrossRef]
26. Buck, H.M.; Cooper, M.A.; Cerny, P.; Grice, J.D.; Hawthorne, F.C. Xenotime-(Yb), $YbPO_4$, a New Mineral Species from the Shatford Lake Pegmatite Group, Southeastern Manitoba, Canada. *Can. Mineral.* **1999**, *37*, 1303–1306.
27. Voloshin, A.V.; Pakhomovsky, Y.A.; Men'shikov, Y.P.; Povarennykh, A.S.; Matvinenko, E.N.; Yakubovich, O.V. Hingganite-(Yb), a new mineral from amazonite pegmatites of the Kola Peninsula. *Dokl. Akad. Nauk SSSR* **1983**, *270*, 1188–1192. (In Russian)
28. Voloshin, A.V.; Pakhomovsky, Y.A.; Tyusheva, F.N. Keiviite $Yb_2Si_2O_7$—A new ytterbium silicate from amazonitic pegmatites of the Kola Peninsula. *Mineral. Zh.* **1983**, *5*, 94–99. (In Russian)
29. Voloshin, A.V.; Pakhomovsky, Y.A. *Minerals and Evolution of Mineral Formation in Amazonitic Pegmatites of the Kola Peninsula*; Nauka: Leningrad, Soviet Union, 1986. (In Russian)
30. Hogarth, D.D.; Chao, G.Y.; Plant, A.G.; Steacy, H.R. Caysichite, a new silico-carbonate of yttrium and calcium. *Can. Mineral.* **1974**, *12*, 293–298.
31. Mellini, M.; Merlino, S. Caysichite: A double crankshaft chain structure. *Can. Mineral.* **1978**, *16*, 81–88.
32. IMA Database of Mineral Properties. Available online: https://rruff.info/ima/# (accessed on 7 September 2025).
33. Nickel, E.H.; Mandarino, J.A. Procedures involving the IMA Commission on New Minerals and Mineral Names and guidelines on mineral nomenclature. *Am. Mineral.* **1987**, *72*, 1031–1042.
34. Bayliss, P.; Levinson, A.A. A system of nomenclature for rare-earth mineral species: Revision and extension. *Am. Mineral.* **1988**, *73*, 422–423.
35. Kristiansen, R. Caysichitt-(Y) og Chernovitt-(Y) fra Lindvikskollen, Kragerø; 2 nye mineraler for Norge. *Stein. Nord. Mag. Popul. Geol.* **1993**, *20*, 125–128.
36. Hori, H.; Kobayashi, T.; Miyawaki, R.; Matsubara, S.; Yokoyama, K.; Shimizu, M. Iwashiroite-(Y), $YTaO_4$, a New Mineral from Suishoyama, Kawamata Town, Fukushima Prefecture, Japan. *J. Mineral. Petrol. Sci.* **2006**, *101*, 170–177. [CrossRef]
37. Palenzona, A.; Martinelli, A.; Pani, M.; Selmi, P. La caysichite-(Y) di Veirera (Gruppo di Voltri, Liguria centrale). *Riv. Mineral. Ital.* **2004**, *28*, 253–255.
38. Wallwork, K.; Kolitsch, U.; Pring, A.; Nasdala, L. Decrespignyite-(Y), a new copper yttrium rare earth carbonate chloride hydrate from Paratoo, South Australia. *Mineral. Mag.* **2002**, *66*, 181–188. [CrossRef]
39. Kuznetsov, S.K.; Onishchenko, S.A. Gold-bearing capacity of local areas of metasomatically altered rhyolites (the Chudnoe deposit in the Subpolar Urals). *Vestnik IG Komi SC UB RAS* **2018**, *12*, 39–45. (In Russian)
40. Habel, M. Der Granodioritbruch der Fa. Josef Uhrmann OHG, Steinerleinbach bei Röhrnbach. *Mineralien-Welt* **2009**, *20*, 66–86.
41. Cairncross, B. Aegirine and associated minerals from Mount Malosa, Malawi. *Rocks Miner.* **2002**, *77*, 31–37. [CrossRef]
42. Voloshin, A.V.; Pakhomovsky, Y.A.; Zezyulina, E.P. Caysichite from amazonitic pegmatites of the Kola peninsula. *Mineral. Zh.* **1986**, *8*, 90–93.
43. Kalashnikov, A.O.; Konopleva, N.G.; Pakhomovsky, Y.A.; Ivanyuk, G.Y. Rare Earth Deposits of the Murmansk Region, Russia—A Review. *Econ. Geol.* **2016**, *111*, 1529–1559. [CrossRef]
44. *CrysAlisPro*, Version 1.171.36.20; Agilent Technologies: Santa Clara, CA, USA, 2012.
45. Sheldrick, G.M. A short history of SHELX. *Acta Crystallogr.* **2008**, *A64*, 112–116. [CrossRef]
46. Hahn, T. (Ed.) *International Tables for Crystallography. Vol. 1. Space-Group Symmetry*; Springer: Dordrecht, The Netherlands, 2005.
47. Gagné, O.C.; Hawthorne, F.C. Comprehensive Derivation of Bond-Valence Parameters for Ion Pairs Involving Oxygen. *Acta Crystallogr. B* **2015**, *71*, 562–578. [CrossRef] [PubMed]
48. Bosi, F.; Hatert, F.; Hålenius, U.; Pasero, M.; Miyawaki, R.; Mills, S.J. On the Application of the IMA−CNMNC Dominant-Valency Rule to Complex Mineral Compositions. *Mineral. Mag.* **2019**, *83*, 627–632. [CrossRef]
49. Hatert, F.; Burke, E.A.J. The IMA–CNMNC dominant-constituent rule revisited and extended. *Can. Mineral.* **2008**, *46*, 717–728. [CrossRef]
50. Hawthorne, F.C.; Gagné, O.C. New Ion Radii for Oxides and Oxysalts, Fluorides, Chlorides and Nitrides. *Acta Crystallogr. B* **2024**, *80*, 326–339. [CrossRef]
51. Smith, J.V.; Brown, W.L. *Feldspar Minerals. Vol. 1. Crystal Structures, Physical, Chemical and Microstructural Properties*; Springer: Berlin/Heidelberg, Germany, 1988.

52. Krivovichev, S.V. Feldspar polymorphs: Diversity, complexity, stability. *Zapiski RMO (Proc. Russ. Miner. Soc.)* **2020**, *149*, 16–66. [CrossRef]
53. Database of Zeolite Structures. Available online: https://www.iza-structure.org/databases/ (accessed on 7 September 2025).
54. Krivovichev, S.V. Structure Description, Interpretation and Classification in Mineralogical Crystallography. *Crystallogr. Rev.* **2017**, *23*, 2–71. [CrossRef]